Monograph:
Billings, S.A. and Yusof, M.I. (1994) Decomposition of Generalised Frequency Response Functions for Non-Linear Systems Using Symbolic Computation. Research Report. ACSE Research Report 525 . Department of Automatic Control and Systems Engineering

Decomposition of Generalised Frequency Response Functions for Non-linear Systems using Symbolic Computation

By

S.A Billings and M.I Yusof

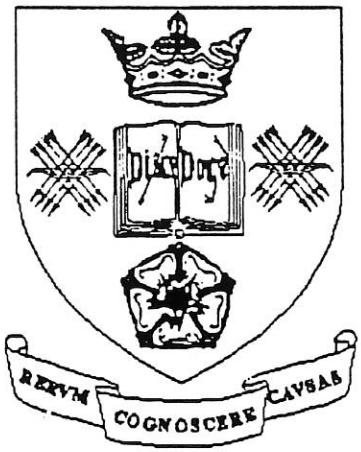

Department of Automatic Control and Systems Engineering

University of Sheffield

Mappin Street

Sheffield S1 4DU

U.K

Research Report No. 525

July 1994

Decomposition of Generalised Frequency Response Functions for Non-linear Systems Using Symbolic Computation

Abstract : *A symbolic manipulation procedure, which both computes and automatically decomposes the generalised frequency response functions of non-linear rational, polynomial and integro-differential equation models into a set of closed-form n-th order transfer functions, is presented. The symbolic representation exposes the explicit relationship between the model parameters and the non-linear transfer functions in the frequency domain and leads to important insights into the characterization of non-linear systems. Examples for each model type are included to demonstrate the symbolic transfer function approach.*

1.0 Introduction

The subject of non-linear systems has attracted a great deal of attention from mathematical scientists in various disciplines ever since the pioneering work by Norbert Wiener in the 1940's. A variety of phenomena, in social and life sciences, the physical sciences, earth sciences and engineering can be accurately described by non-linear equations which may take the form of either algebraic, functional, differential or difference equations. These various model representations play an important role in the common-sense understanding of the physical world around us. Traditionally computational procedures based on these models have almost exclusively involved numerical processing. These computations provide an evaluation of the functions in terms of numerical values which can be plotted or manipulated but the relationship to the original model is not transparent. It is therefore becoming apparent that a new methodology which involves the integration of numerical processing and symbolic reasoning will be very useful. The wide availability of symbolic algebraic languages such as those provided by MACSYMA, Maple and *Mathematica* provide the possibility of symbolic manipulation regardless of the complexity of the mechanism. This means that problems which previously could only be tackled using numerical simulation and analysis can now be solved analytically. All the necessary algebraic manipulations, substitutions, changes of variables and other simplification steps that would normally be carried out by an engineer can now be performed on the computer. Symbolic computing techniques provide a powerful tool kit that can be used to explain the behaviour captured by non-linear models.

The analysis and design of linear systems in the frequency domain is now an established part of systems theory. When the system is non-linear these ideas can extended to higher order or generalised frequency response function(FRF's) which can be estimated from measured signals by extending the classical FFT, windowing and smoothing techniques to many dimensions(Vinh et al, 1987, Kim and Powers,1988, Cho, Kim, Hixson and Powers, 1992). While these approaches have been succesfully applied they often require an

polynomial and NIDE model into the frequency domain is described. Section 5 demonstrates how the generalised FRF's can be decomposed using symbolic manipulations. Key theorems for the development of the new analysis procedures are provided by decomposing the higher order transfer functions into a series combination of lower order transfer functions. By using log plots in section 6, the multiplication/division of gain and phase in the higher order transfer functions can be converted into addition/subtraction and this makes the analysis and interpretation of the FRF's much easier. The phase decomposition of the generalised FRF's using phase unwrapping techniques is discussed in section 6.1. Finally simulated examples are presented to illustrate the application of the new algorithms

2.0 Mathematical Foundation of Generalised FRF's

Traditionally, the input/output behaviour of a wide class of non-linear systems can be represented by the Volterra series

$$y(t) = \sum_{n=1}^{\infty} y_n(t) \tag{1}$$

where $y_n(t)$, the n-th order output of the system, is given by

$$y_n(t) = \int_{-\infty}^{+\infty} \cdots \int_{-\infty}^{+\infty} h_n(\tau_1 \ldots \tau_n) \prod_{i=1}^{n} u(t-\tau_1) d\tau_i \quad n > 0 \tag{2}$$

and $h_n(\bullet)$ is known as the n-th order Volterra kernel or generalised impulse response function of order n. This reduces to the linear impulse response function $h(\tau)$ for n=1. The multidimensional Fourier transform can be applied directly to $h_n(\bullet)$ to yield the n-th order transfer function $H_n(j\omega_1 \ldots j\omega_n)$ or n-th order generalised or higher order FRF defined as

$$H_n(j\omega_1 \ldots j\omega_n) = \int_{-\infty}^{+\infty} \cdots \int_{-\infty}^{+\infty} h_n(\tau_1 \ldots \tau_n) e^{-j(\omega_1\tau_1 + \ldots + \omega_n\tau_n)} d\tau_1 \ldots d\tau_n \tag{3}$$

The Fourier transform pair of eqn(3) can be expressed as

$$h_n(\tau_1, \ldots \tau_n) = \frac{1}{(2\pi)^n} \int \cdots \int_{-\infty}^{+\infty} H_n(j\omega_1 \ldots j\omega_n) \times e^{j(\omega_1 + \ldots + \omega_n)t} d\omega_1 \ldots d\omega_n \tag{4}$$

By substituting (4) into (2) and carrying out the multiple integration on $\tau_1, \ldots \tau_n$ gives the n-th order output of the system

$$y_n(t) = \frac{1}{(2\pi)^n} \sum_{n=1}^{\infty} \int_{-\infty}^{+\infty} \cdots \int_{-\infty}^{+\infty} H_n(j\omega_1 \ldots j\omega_n) \prod_{i=1}^{n} U(j\omega_i) e^{j(\omega_1 + \ldots + \omega_n)t} d\omega_i \tag{5}$$

where $U(j\omega_i)$ represents the input spectrum. When the system has a non-zero steady state for zero input the behaviour of the non-linear system can be described by adding a degree-0 term y_0 into the Volterra series in eqn(1) (Peyton et al, 1992). This accommodates mean levels in the measured signals of the process. The output can then be expressed as

$$y(t) = y_0 + \sum_{n=1}^{N} y_n(t) \tag{6}$$

Substituting (2) into (6) yields the following general expression

$$y(t) = y_0 + \sum_{n=1}^{N} \int_{-\infty}^{+\infty} \cdots \int_{-\infty}^{+\infty} h_n(\tau_1 \ldots \tau_n) \prod_{i=1}^{n} u(t-\tau_1) d\tau_i \tag{7}$$

The output $y(t)$ can be simplified by using the probing method to expand the equation for complex exponential inputs (Bedrosian and Rice, 1971)

$$u(t) = \sum_{r=1}^{R} e^{j\omega_r t} \tag{8}$$

to yield

$$\begin{aligned} y(t) &= y_0 + \sum_{n=1}^{N} \int_{-\infty}^{+\infty} \cdots \int_{-\infty}^{+\infty} h_n(\tau_1 \ldots \tau_n) \prod_{i=1}^{n} \sum_{r=1}^{R} e^{j\omega_r t} d\tau_i \\ &= y_0 + \sum_{n=1}^{N} \sum_{r_1 \ldots r_n=1}^{R} \left[\int_{-\infty}^{+\infty} \cdots \int_{-\infty}^{+\infty} h_n(\tau_1 \ldots \tau_n) \prod_{i=1}^{n} e^{-j\omega_{r_i}\tau_i} d\tau_i \right] e^{j(\omega_{r_1} + \ldots + \omega_{r_n})t} \\ &= H_0 + \sum_{n=1}^{N} \sum_{r_1 \ldots r_n=1}^{R} H_n(j\omega_{r_1}, \ldots, j\omega_{r_n}) e^{j(\omega_{r_1} + \ldots + \omega_{r_n})t} \end{aligned} \tag{9}$$

where H_0 is associated with the 0 order output y_0 which is independent of any input and $H_n(j\omega_{r_1}, \ldots, j\omega_{r_n})$ can be recognised as the non-linear transfer function. Note that in general $h_n(\tau_1 \ldots \tau_n)$ and the associated transform $H_n(j\omega_{r_1}, \ldots, j\omega_{r_n})$ may not be symmetric functions of their arguments. That is the order of arguments in $h_n(\bullet)$ or $H_n(\bullet)$ cannot be interchanged. Inspection of eqn(7) shows that the output $y_n(t)$ will be identical for any permutation of the arguments. All kernels that differ only by the permutation of their arguments are therefore equivalent representations of the system. Consequently we can arbitrarily replace any kernel by $1/n!$ times the sum of all the $n!$ kernels resulting from all the permutations of the arguments to yield symmetric kernels. The advantages of the symmetric form of the Volterra kernels is that they are unique(the asymmetric form is non-unique) and the convenience for manipulation because the order of the τ's is unimportant. Because any symmetric kernel can be symmetrized using the procedure described, there is no loss of generality by considering only symmetry kernels. Thus the symmetrized n-th order frequency response function is defined by

$$H_n^{Sym}(j\omega_1 \ldots j\omega_n) = \frac{1}{n!} \sum_{\substack{\text{all permutations} \\ \text{of } \omega_1 \ldots \omega_n}} H_n(j\omega_1 \ldots j\omega_n) \tag{10}$$

A wide class of non-linear systems can be characterized using the generalised FRF's providing estimates of these are available. Estimation using FFT based techniques has been widely studied and documented(Kim and Powers,1988, Cho, Kim, Hixson and Powers, 1992) but only the parametric estimation approach will be considered in the present study because this provides the models which form the basis of the symbolic expansions.

3.0 Parametric Estimation of Generalised FRF's

3.1 The Non-linear Rational Model

Consider the non-linear dynamic discrete-time rational model which is a superset of the polynomial model and which can be derived as a particular expansion of the NARMAX model (Chen and Billings, 1989)

$$y(t)=\frac{a(y(t-1),\ldots y(t-k),u(t-1),\ldots u(t-k),\zeta(t-1),\ldots\zeta(t-k))}{b(y(t-1),\ldots y(t-k),u(t-1),\ldots u(t-k),\zeta(t-1),\ldots(t-k))}+\zeta(t) \tag{11}$$

where $y(t)$ and $u(t)$ represent the output and input at time $t(t=1,2,\ldots)$ respectively, k is maximum lag of the model, $\zeta(t)$ is an unobservable independent and identically distributed noise with zero mean and finite variance σ_ε^2, and $a(\bullet)$ and $b(\bullet)$ are used to denote polynomials in the numerator and denominator respectively. Algorithms for detecting the model structure, estimating the parameters, and validating the models are available in the literature(Chen and Billings, 1989, Zhu and Billings, 1991, Billings and Zhu, 1992). Once the identification process is complete, the noise terms, which are included to ensure unbiased estimation, are discarded to yield a deterministic 'NARX(Non-linear AutoRegressive with eXogenous inputs) model containing input and output terms only.

The resulting rational non-linear rational NARX model with a constant term $\alpha_{0,0}$ can be expressed in the general form as

$$y(t)=\frac{\alpha_{0,0}+Y_a(t;\theta_a,y,u)}{Y_b(t;\theta_b,y,u)} \tag{12}$$

where $Y_a(t;\theta_a,y,u)$ and $Y_b(t;\theta_b,y,u)$ may be viewed as an expansion of polynomials in the numerator and denominator respectively defined as

$$Y_a(t;\theta_a,y,u)=\sum_{m=1}^{M_a}\left[\sum_{p=0}^{m}\sum_{k_1\ldots k_{p+q}=1}^{k_a}\alpha_{p,q}(k_1,\ldots k_{p+q})\prod_{i=1}^{p}y(t-k_i)\prod_{i=p+1}^{p+q}u(t-k_i)\right] \tag{13}$$

and

$$Y_b(t;\theta_b,y,u)=\sum_{m=0}^{M_b}\left[\sum_{p=0}^{m}\sum_{k_1\ldots k_{p+q}=1}^{k_b}\beta_{p,q}(k_1,\ldots k_{p+q})\prod_{i=1}^{p}y(t-k_i)\prod_{i=p+1}^{p+q}u(t-k_i)\right] \tag{14}$$

where M_a and M_b denote the maximum degrees of nonlinearities, k_a and k_b are the maximum lags in the input or output in the numerator and denominator respectively. $\alpha(\bullet)$ and $\beta(\bullet)$ are the parameters associated with the various terms in the two polynomials(corresponding to the parameter set θ_a and θ_b respectively), $p+q=m$ and

$$\sum_{k_1\ldots k_n=1}^{k}\equiv\sum_{k_1=1}^{k}\cdots\sum_{k_n=1}^{k}$$

Notice that, the standard polynomial NARX model is just a special case of eqn(12) given by setting $Y_b(t;\theta_b,y,u)=1$.

For example a simple rational model of the form

$$y(t)=\frac{2.0+1.98y(t-1)+0.01y(t-1)u(t-1)}{0.9+u^2(t-1)} \tag{15}$$

can be described by eqn(12) with the following assignments

$$\alpha_{0,0} = 2.0,\ \alpha_{1,0}(1) = 1.98,\ \alpha_{1,1}(1,1) = 0.01,\ \beta_{0,0} = 0.9,\ \beta_{0,2}(1,1) = 1.0 \qquad (16)$$
$$k_a = k_b = 1,\ M_a = 1 \text{ and } M_b = 2$$

3.2 Mapping the Non-linear Rational Model into the Frequency Domain

Generalised FRFs of any order can be obtained by mapping the non-linear rational model into the frequency domain(Billings and Tsang, 1989a, Peyton-Jones and Billings, 1989).

Consider the general representation of a non-linear time domain model

$$M(t;\theta,y,u) + \alpha_{0,0} = 0 \qquad (17)$$

where $M(\bullet)$ is a functional series in terms of the output $y(t)$, input $u(t)$, $\alpha_{0,0}$ is a constant term and θ is the set of model parameters. In the discrete-time case, u and y contain both the current and previous sampled values so that

$$u \equiv \{u(t), u(t-1), \ldots\}$$
$$y \equiv \{y(t), y(t-1), \ldots\}$$

The generalised frequency response function $H_n(\bullet)$ can then be obtained by substituting the Volterra series eqn(9) to replace y in $M(\bullet)$ to yield

$$M(t;\theta,H,\omega_r) + \alpha_{0,0} = 0 \qquad (18)$$

where $H \equiv \{H_0, H_1, \ldots, H_N\}$ and ω_r implies $\{\omega_1 \ldots \omega_r\}$. Introducing the operator $\mathcal{E}_n(\bullet)$ to denote the operation of extracting the coefficient of $e^{j(\omega_1+\ldots+\omega_n)t}$, the following harmonic expansion is obtained(Zhang, Billings and Zhu, 1993)

$$\mathcal{E}_n\left[M(t;\theta,H,\omega_r) + \alpha_{0,0}\right] = 0 \qquad (19)$$

This forms the basis of a recursive algorithm for determining the generalised FRFs from rational models (Zhang, Billings and Zhu, 1993). The rational model is first probed using a single complex exponential $e^{j\omega_1 t}$. This permits the determination of the linear transfer function $H_1(j\omega_1)$. The probing is then extended to the sum of two complex exponentials, given by $e^{j\omega_1 t} + e^{j\omega_2 t}$, to yield $H_2(j\omega_1, j\omega_2)$. This procedures continues with one additional complex exponential being added to the input at each step so that at step n the input consists of the sum $e^{j\omega_1 t} + \ldots + e^{j\omega_n t}$. The non-linear transfer function of order n is constructed from all of the previously determined lower order non-linear transfer functions. Clearly the computation can rapidly become cumbersome as the order increases, even for mildly non-linear systems. Hence an easier and more efficient approach needs to be formulated when dealing with severe-nonlinearites. This can be achieved for the non-linear rational model by using the algorithm derived by Zhang, Billings and Zhu, (1993).

Rewriting eqn(12) the rational model can be expressed as

$$M(\bullet) = \alpha_{0,0} + Y_a(t;\theta_a,y,u) - Y_b(t;\theta_b,y,u)y(t) = 0 \qquad (20)$$

The desired frequency response functions $H_n(\bullet)$ for this model, which includes the polynomial NARMAX model as a special case, can then be found by applying the operator $\mathcal{E}_n(\bullet)$ to the model expression $M(\bullet)$ according to eqn(19).The final algorithm for computing n-th order generalised FRF's takes the form (Billings et al, 1994)

$$\begin{aligned}
&\Big(\beta_{0,0}-\sum_{p=1}^{M_a}\sum_{k_1,k_p=1}^{k_a}\alpha_{p,0}(k_1,\ldots,k_p)H_0^{p-1}\times\sum_{i=1}^{p}e^{-j(\omega_1+\ldots+\omega_n)k_i}+\\
&\sum_{p=1}^{M_b}\sum_{k_1,k_p=1}^{k_a}\beta_{p,0}(k_1,\ldots,k_p)H_0^{p}\times\left(\sum_{i=1}^{p}e^{-j(\omega_1+\ldots+\omega_n)k_i}+1\right)\Big)H_n^{usym}(j\omega_1,\ldots,j\omega_n)=\\
&\quad\sum_{k_1,k_n=1}^{K_a}\alpha_{0,n}(k_1,\ldots,k_n)e^{-j(\omega_1k_1+\ldots+\omega_nk_n)}\\
&\quad+\sum_{p=2}^{M_a}\sum_{k_1,k_p=1}^{K_a}\alpha_{p,0}(k_1,\ldots,k_p)\,{}^{D}\overline{H}_{n,p}(\bullet)\\
&\quad+\sum_{q=1}^{n}\sum_{p=1}^{M_a-1}\sum_{k_1,k_{p+q}=1}^{K_a}\alpha_{p,q}(k_1,\ldots,k_{p+q})e^{-j(\omega_{n-q+1}k_{p+1}+\ldots+\omega_nk_{p+q})}\,{}^{D}H_{n-q,p}(\bullet)\\
&\quad-\sum_{q=1}^{n}\sum_{k_1,k_q=1}^{K_b}\beta_{0,q}(k_1,\ldots,k_q)e^{-j(\omega_{n-q+1}k_1+\ldots+\omega_nk_q)}H_{n-q}(\bullet)\\
&\quad-\sum_{p=1}^{M_b}\sum_{k_1,k_p=1}^{K_b}\beta_{p,0}(k_1,\ldots,k_p)\,{}^{D}\overline{H}_{n,p+1}^{usym}(\bullet)\\
&-\sum_{q=1}^{n}\sum_{p=1}^{M_b-1}\sum_{k_1,k_{p+q}=1}^{K_b}\beta_{p,q}(k_1,\ldots,k_{p+q})e^{-j(\omega_{n-q+1}k_{p+1}+\ldots+\omega_nk_{p+q})}\,{}^{D}\overline{H}_{n-q,p+1}(\bullet)
\end{aligned}\tag{21}$$

The recursive relations ${}^{D}H_{n,p}(\bullet)$ are given by

$${}^{D}H_{n,p}^{usym}(\bullet)=\sum_{i=0}^{n}H_i^{usym}(j\omega_1,\ldots,j\omega_i)\,{}^{D}H_{n-i,p-1}(j\omega_{i+1},\ldots,j\omega_n)e^{-j(\omega_1+\ldots+\omega_i)k_p}\tag{22}$$

Note that the recursion ends with $p=1$, ${}^{D}H_{n,1}(j\omega_1,\ldots,j\omega_n)$ is given as

$${}^{D}H_{n,1}(j\omega_1,\ldots,j\omega_n)=H_n(j\omega_1,\ldots,j\omega_n)e^{-j(\omega_1+\ldots+\omega_n)k_1}\tag{23}$$

and ${}^{D}\overline{H}_{n,p}(\bullet)$is a subset of ${}^{D}H_{n,p}(\bullet)$, defined by excluding all the terms of $H_n(\bullet)$in the expansion of eqn(22). For example the expansion of ${}^{D}H_{2,4}(j\omega_1,j\omega_2)$using eqns (22) and (23) is given as

$$\begin{aligned}
{}^{D}H_{2,4}(j\omega_1,j\omega_2)=H_0^3H_2(j\omega_1,j\omega_2)\sum_{i=1}^{4}e^{-j(\omega_1+\omega_2)k_i}\\
H_0^2H_1(j\omega_1)H_1(j\omega_2)\Big[e^{-j(\omega_1k_4+\omega_2k_1)}+e^{-j(\omega_1k_4+\omega_2k_2)}+e^{-j(\omega_1k_4+\omega_2k_3)}\\
e^{-j(\omega_1k_2+\omega_2k_1)}+e^{-j(\omega_1k_3+\omega_2k_1)}+e^{-j(\omega_1k_3+\omega_2k_2)}\Big]
\end{aligned}$$

and ${}^{D}\overline{H}_{2,4}(j\omega_1,j\omega_2)$ is obtained by excluding all the terms of $H_2(\bullet)$

$$\begin{aligned}
{}^{D}\overline{H}_{2,4}(j\omega_1,j\omega_2)=H_0^2H_1(j\omega_1)H_1(j\omega_2)\Big[e^{-j(\omega_1k_4+\omega_2k_1)}+e^{-j(\omega_1k_4+\omega_2k_2)}+e^{-j(\omega_1k_4+\omega_2k_3)}\\
e^{-j(\omega_1k_2+\omega_2k_1)}+e^{-j(\omega_1k_3+\omega_2k_1)}+e^{-j(\omega_1k_3+\omega_2k_2)}\Big]
\end{aligned}$$

Setting the input to zero the initial condition H_0 can computed from the resultant steady state equation

$$\beta_{0,0}H_0-\alpha_{0,0}-\sum_{p=1}^{M_a}\sum_{k_1,k_p=1}^{k_a}\alpha_{p,0}(k_1,\ldots,k_{p+q})H_0^p+\sum_{p=1}^{M_b}\sum_{k_1,k_p=1}^{k_b}\beta_{p,0}(k_1,\ldots,k_{p+q})H_0^{p+1}=0 \qquad (24)$$

It seen that $\alpha_{0,0}$ is the only constant term in the above equation. Notice that there may be more than one solution for H_0 which implies that the underlying system may exhibit multiple steady state solutions. If $\alpha_{0,0}$=0, that is if the numerator polynomial in eqn(12) does not contain a constant term, H_0 will be zero. Finally it is worth noting that the generalised FRF for the standard polynomial NARMAX model is just a special case of eqn(21) given by setting all the coefficients $\beta_{(\bullet)}(\bullet)=0$ except $\beta_{0,0}=1$ or setting $Y_b(\bullet)=1$ in equation(12).

Inspection of equation (21), shows that the first few generalised FRF's with maximum nonlinearity $M_a=5$ and $M_b=4$ can be written as

$$H_1^{asym}(j\omega_1)=\frac{\left(\sum_{k_1}^{k_a}\alpha_{0,1}(k_1)e^{-j(\omega_1k_1)}+\sum_{p=2}^{5}\sum_{k_1,k_p=1}^{k_a}\alpha_{p,0}(k_1,\ldots,k_p)\,{}^{D}\overline{H}_{1,p}(\bullet)+\right.}{\left.\sum_{p=1}^{4}\sum_{k_1,k_{p+q}=1}^{k_a}\alpha_{p,q}(k_1,\ldots k_{p+q})e^{-j(\omega_1k_{p+1})}\,{}^{D}H_{0,p}(\bullet)-\sum_{k_1,k_{p+q}=1}^{k_a}\beta_{0,q}(k_1,\ldots k_q)e^{-j(\omega_1k_1)}H_0\right)}$$
$$\frac{}{\left(\beta_{0,0}-\sum_{p=1}^{M_a}\sum_{k_1,k_p=1}^{k_a}\alpha_{p,0}(k_1,\ldots,k_p)H_0^{p-1}\times\sum_{i=1}^{p}e^{-j(\omega_1)k_i}+\sum_{p=1}^{M_b}\sum_{k_1,k_p=1}^{k_b}\beta_{p,0}(k_1,\ldots,k_p)H_0^p\left(\sum_{i=1}^{p}e^{-j(\omega_1)k_i}+1\right)\right)}$$

$$H_2^{asym}(j\omega_1,j\omega_2)=\frac{\left(\sum_{k_1,k_2=1}^{k_a}\alpha_{0,2}(k_1,\ldots,k_5)e^{-j(\omega_1k_1+\omega_2k_2)}+\sum_{p=2}^{5}\sum_{k_1,k_p=1}^{k_a}\alpha_{p,0}(k_1,\ldots,k_p)\,{}^{D}\overline{H}_{2,p}(\bullet)\right.}{+\sum_{q=1}^{2}\sum_{p=1}^{2}\sum_{k_1,k_{p+q}=1}^{k_a}\alpha_{p,q}(k_1,\ldots k_{p+q})e^{-j(\omega_{3-q}k_{p+1}+\ldots+\omega_2k_{p+q})}\,{}^{D}H_{2-q,p}(\bullet)}$$
$$-\sum_{q=1}^{2}\sum_{k_1,k_q=1}^{k_b}\beta_{0,q}(k_1,\ldots k_q)e^{-j(\omega_{3-q}k_1+\ldots+\omega_2k_q)}H_{2-q}(\bullet)$$
$$-\sum_{p=1}^{4}\sum_{k_1,k_p=1}^{k_b}\beta_{p,0}(k_1,\ldots k_p)\,{}^{D}\overline{H}_{2,p+1}^{asym}(\bullet)$$
$$\left.-\sum_{q=1}^{2}\sum_{p=1}^{2}\sum_{k_1,k_{p+q}=1}^{k_b}\beta_{p,q}(k_1,\ldots k_{p+q})e^{-j(\omega_{3-q}k_{p+1}+\ldots+\omega_2k_{p+q})}\,{}^{D}\overline{H}_{2-q,p+1}(\bullet)\right)$$
$$\frac{}{\left(\beta_{0,0}-\sum_{p=1}^{M_a}\sum_{k_1,k_p=1}^{k_a}\alpha_{p,0}(k_1,\ldots,k_p)H_0^{p-1}\times\sum_{i=1}^{p}e^{-j(\omega_1+\omega_2)k_i}+\sum_{p=1}^{M_b}\sum_{k_1,k_p=1}^{k_b}\beta_{p,0}(k_1,\ldots,k_p)H_0^p\times\left(\sum_{i=1}^{p}e^{-j(\omega_1+\omega_2)k_i}+1\right)\right)}$$

$$\bullet$$
$$\bullet$$
$$\bullet$$

processing which would quickly become overwhelming for the more complex rational models which are typically obtained from system identification, it becomes a necessity to consider an alternative approach. Symbolic processing, which will be considered in section 5.0, provides the ideal solution because of the flexibility allowed and more importantly because the analytic form of the expressions are provided and these significantly aid interpretation.

4.0 The Non-linear Integro-Differential Equation Model

It is also important to consider how continuous time non-linear models can be mapped into the frequency domain. A polynomial structure for a broad class non-linear integro differential models may be represented as

$$\sum_{m=1}^{M}\sum_{p=0}^{m}\sum_{l_1,l_{p+q}=-L}^{L} c_{p,q}(l_1,\ldots,l_{p+q})\prod_{i=1}^{p} D^{l_i}y(t)\prod_{i=p+1}^{p+q} D^{l_i}u(t)+C_0=0 \tag{28}$$

where $p+q=m$, $c_{p,q}(l_1,\ldots,l_{p+q})$ denotes the parameter associated with the p-th order nonlinearity in $D^{l_i}y(t)$ and the q-th order nonlinearity in $D^{l_i}u(t)$, and the D operator is defined by

$$D^{l}x(t)=\begin{cases}\dfrac{d^{l}x(t)}{dt^{l}} & \\ \int_{-\infty}^{t}\ldots\int_{-\infty}^{\tau_2} x(\tau_1)d\tau_1\ldots d\tau_{|l|} & l<0\end{cases} \tag{29}$$

Consider for example a specific instance of the NIDE model with a constant term

$$D^2y(t)+\left(1-y(t)^2\right)Dy(t)+y(t)+10-u(t)=0 \tag{30}$$

This may be obtained from the general form eqn(28) by defining the coefficients as

$$c_{1,0}(2)=1.0 \qquad c_{1,0}(1)=1.0 \qquad c_{3,0}(0,0,1)=-1.0$$
$$c_{1,0}(0)=1.0 \qquad C_0=10 \qquad c_{0,1}(0)=-1.0 \qquad else \quad c_{p,q}(\bullet)=0; \tag{31}$$

4.1 Mapping the NIDE model into the Frequency Domain

Peyton-Jones and Billings, (1992) showed that the n-th order generalised FRF of the NIDE in eqn(28) is given by

$$-\left(\sum_{p=1}^{M}\sum_{l_1 l_p=-L}^{L} c_{p,0}(l_1,\ldots l_p)H_0{}^{p-1}\times\sum_{i=1}^{p}(j\omega_1+\ldots+j\omega_n)^{l_i}\right)H_n{}^{sym}(j\omega_1,\ldots,j\omega_n)=$$
$$\sum_{l_1,l_n=-L}^{L} c_{0,n}(l_1,\ldots,l_n)(j\omega_1)^{l_1}\ldots(j\omega_n)^{l_n}$$
$$+\sum_{q=1}^{n}\sum_{p=1}^{M-1}\sum_{l_1,l_{p+q}=-L}^{L} c_{p,q}(l_1,\ldots,l_{p+q})(j\omega_{n-q+1})^{l_{p+1}}\ldots(j\omega_n)^{l_{p+q}}\ {}^{c}H_{n-q,p}(j\omega_1,\ldots,j\omega_{n-q})$$
$$+\sum_{p=1}^{M}\sum_{l_1,l_p=-L}^{L} c_{p,0}(l_1,\ldots,l_p)\ {}^{c}\overline{H}_{n,p}(j\omega_1,\ldots,j\omega_n)$$

$$H_5^{asym}(j\omega_1,\ldots,j\omega_5) = \sum_{l_1,l_n=-L}^{L} c_{0,5}(l_1,\ldots,l_5)(j\omega_1)^{l_1}\ldots(j\omega_5)^{l_5}$$
$$+\sum_{q=1}^{5}\sum_{p=1}^{4}\sum_{l_1,l_{p+q}=-L}^{L} c_{p,q}(l_1,\ldots,l_{p+q})(j\omega_{5-q+1})^{l_{p+1}}\ldots(j\omega_5)^{l_{p+q}}\ {}^{c}H_{5-q,p}(j\omega_1,\ldots,j\omega_{5-q})$$
$$+\sum_{p=1}^{5}\sum_{l_1,l_p=-L}^{L} c_{p,0}(l_1,\ldots,l_p)\,{}^{c}\overline{H}_{5,p}(j\omega_1,\ldots,j\omega_5)$$
$$-\left(\sum_{p=1}^{5}\sum_{l_1,l_p=-L}^{L} c_{p,0}(l_1,\ldots l_p)H_0{}^{p-1}\times\sum_{i=1}^{p}(j\omega_1+j\omega_2+j\omega_3+j\omega_4+j\omega_5)^{l_i}\right) \qquad (36)$$

The asymmetric generalised FRF $H_n^{asym}(j\omega_1,\ldots,j\omega_n)$ can be converted into symmetrised form using equation (26) and the properties mentioned in equation (27).

5.0 Symbolic Computation of the Generalised Frequency Response Functions

Several researchers(Evans, Karam, Kevin and McCellan, 1993, Nethery and Spong, 1994) have investigated symbolic signal processing procedures where the computer manipulates a formula rather than a sequence of numbers. Maintaining the signal processing operators in symbolic form enables machines to simplify, rearrange and rewrite the symbolic expressions until they take a desired form.

The generalised FRF's are an important mechanism for investigating the behaviour of non-linear dynamical systems(Chua and Ng, 1979a, 1979b, Billings and Tsang, 1989a, 1989b) and symbolic expressions for these in terms of the time domain model parameters would considerably aid their interpretation and understanding. Closed form expressions for the generalised FRF's of any order for both discrete time and continuous time NIDE have been given above. The derivation of the mathematical expressions for $H_1(j\omega_1)$, $H_2(j\omega_1,j\omega_2)$, $H_3(j\omega_1,j\omega_2,j\omega_3)$ etc for even very simple model forms is clearly very complex (Peyton-Jones and Billings, 1989, Zhang, Billings and Zhu, 1993) and rarely attempted for anything other than trivial models and then only up to n=3. Symbolic processing of the generalised FRFs would therefore seem to offer enormous potential. Analytic forms of the transfer functions could be inspected and if required specific model parameter values could be inserted to produce numerical or graphical output.

In symbolic processing computer algebra, computational geometry, automated reasoning, and automatic programming are utilised. The main task in the derivation and analysis of generalised FRF's is the manipulation of elementary functions by powerful pattern matching methods including conditional rules. This permits the development of complex rule bases

functions to decompose them into easy to interpret components and to show how these components combine and interact to produce the overall FRF's.

Applying the same argument, the phase decomposition is obtained as

$$\arg\left|H_n(j\omega_1,\ldots j\omega_n)\right| = \arg\left|P(j\omega_1,\ldots j\omega_n)\right| - \arg\left|Q(j\omega_1,\ldots j\omega_n)\right| \tag{39}$$

However to use this transformation, the ambiguity of the argument must first be removed and then only general superposition can be satisfied. The ambiguity of the argument is removed by considering the principal value modulo 2π. This cannot be employed here and as a result phase unwrapping will be used as an alternative.

6.1 Phase Unwrapping:The Integration Approach

Several numerical schemes have been proposed to unwrap the phase spectrum for the linear systems case(Tribolet, 1977, Mc Gowan and Kuc, 1982). These ideas were extending to the generalised FRF case which is required for non-linear systems by Zhang and Billings(1993). The approach adopted here is based upon the so called numerical integration scheme. This scheme combines the information contained in both the derivatives and the principal values of the phase. Initially two dimensional phase unwrapping is derived by extending the results from the one dimensional case. The phase response can be defined as

$$\arg\left[H(j\omega)\right] \triangleq \tan^{-1}\frac{\mathrm{Im}\left[H(j\omega)\right]}{\mathrm{Re}\left[H(j\omega)\right]} \tag{40}$$

To remove the ambiguity and hence the discontinuous jumps in the traditional phase plots at $\pm 180^{\circ}$ and at the same time to satisfy eqn(39) the argument $\arg\left[H_n(\bullet)\right]$ must be defined so that it is a continuous function of $H_n(\bullet)$. Using the principal value however(Zhang and Billings, 1993) can introduce artificial discontinuities of 2π making it impossible to measure the net change of phase in $H_n(\bullet)$ as the frequency variables $\{\omega_1\ldots\omega_n\}$ go from 0 to ∞ (0 to 2π for discrete systems). This problem can be addressed by defining an unwrapped phase function $\phi(\omega_1)$ as the integral of the phase derivative. For notational reasons it is convenient to define

$$H_R(\omega) \triangleq \mathrm{Re}\left[H(j\omega)\right];\ H_I(\omega) \triangleq \mathrm{Im}\left[H(j\omega)\right] \tag{41}$$

hence

$$\phi(\omega_2) \triangleq \tan^{-1}\frac{H_I(j\omega)}{H_R(j\omega)} \tag{42}$$

Then by formally computing the derivative of the right hand side of equation (40) and equating this to the derivative of $\phi(\omega_2)$ yields

$$\frac{d\phi(\omega_2)}{d\omega_2} = \frac{H_R(\omega_2)\dfrac{dH_I(\omega_2)}{d\omega_2} - H_I(\omega_2)\dfrac{dH_R(\omega_2)}{d\omega_2}}{H_R^2(\omega_2)+H_I^2(\omega_2)} \tag{43}$$

The two derivatives, $H_I^{'}(\bullet)$and $H_R^{'}(\bullet)$ are obtained by perturbing the frequency variable ω with a small deviation, that is

$$H_R^{'}(\omega)=\frac{H_R(\omega+\Delta\omega)-H_R(\omega)}{\Delta\omega};\qquad H_I^{'}(\omega)=\frac{H_I(\omega+\Delta\omega)-H_I(\omega)}{\Delta\omega} \tag{44}$$

$\Delta\omega=0.001$ was used in the present analysis. All the values of $H_R(\bullet)$and $H_I(\bullet)$ are directly extracted from the complex value of $H(j\omega)$. The phase derivative can now be computed using eqn.(43). The unwrapped phase function $\phi(\nu_2)$at a particular frequency ν_2 can then be evaluated at any given frequency ω by integrating the derivative

$$\phi(\nu_2)=\phi(\omega_0)+\int_{\omega_0}^{\nu_2}\frac{d\phi(\omega_2)}{d\omega_2}d\omega_2 \tag{45}$$

To obtain the unwrapped phase on a given sequence of frequency values ω_k, $k=1,2,3,4\ldots,N$, along the frequency axis the unwrapped value at each ω_k can be evaluated separately, all from the initial point defined in this case as $\omega_0=0$. Two dimensional phase unwrapping algorithms can be derived by considering the second order generalised phase response in detail. The extension to higher order generalised frequency response functions is obtained by increasing the number of dimensions(Zhang and Billings, 1993). Consider the 2D unwrapped phase function as an extension of the one-dimensional unwrapped phase

$$\phi(\nu_1,\nu_2)=\phi(\omega_{10},\omega_{20})+\int_{\omega_{10}}^{\nu_2}\frac{\partial\phi(\omega_{10},\omega_2)}{\partial\omega_2}d\omega_2+\int_{\omega_{20}}^{\nu_1}\frac{\partial\phi(\omega_1,\nu_2)}{\partial\omega_1}d\omega_1 \tag{46}$$

where the partial derivatives are given by formulas analogous to (43)

$$\partial\phi(\omega_{10},\omega_2)=\frac{H_R(\omega_{10},\omega_2)\dfrac{\partial H_I(\omega_{10},\omega_2)}{\partial\omega_2}-H_I(\omega_{10},\omega_2)\dfrac{\partial H_R(\omega_{10},\omega_2)}{\partial\omega_2}}{\left|H(j\omega_{10},j\omega_2)\right|^2} \tag{47}$$

and

$$\partial\phi(\omega_1,\nu_2)=\frac{H_R(\omega_1,\nu_2)\dfrac{\partial H_I(\omega_1,\nu_2)}{\partial\omega_1}-H_I(\omega_1,\nu_2)\dfrac{\partial H_R(\omega_1,\nu_2)}{\partial\omega_1}}{\left|H(j\omega_1,j\nu_2)\right|^2} \tag{48}$$

The numerical integration in eqn(46) can then be evaluated to give the unwrapped phase response value $\phi(\nu_1,\nu_2)$at any point (ν_1,ν_2). The initial point $(\omega_{10},\omega_{20})$ can be taken as the origin (0,0) or chosen arbitrarily. The selection of the initial point may affect the integration time and probably the relative position of the resulting phase surface. Although results obtained with different initial points may differ from each other by 2π they will have the same shape. In order to get a 3D mesh surface for the unwrapped phase response, the two frequency axes are each sampled to form an $N\times M$ grid. A 3D graphical surface can then be obtained by computing the unwrapped phase value at every point on the frequency axis denoted by $[\omega_1(i),\omega_2(k)]$ with $i=1,\ldots N$ and $k=1,\ldots M$.

7.0 Examples

7.1 A Rational Model Example

Consider the rational NARX model which is represent by

$$y(t)=\frac{0.9004y(t-1)-y(t-2)+0.001u(t-0)}{0.9979+0.002097y^2(t)-0.001097y(t)y(t-1)} \tag{49}$$

The sampling frequency in this case was 1KHz. The parameters of the rational model can be coded to conform with eqn(12) as follows

$\alpha_{1,0}(1)=0.9004;\ \alpha_{1,0}(2)=-1.0000;\ \alpha_{0,1}(0)=0.001;$

$\beta_{0,0}=0.9979;\ \beta_{2,0}(0,0)=0.002097;\ \beta_{2,0}(1,0)=-0.001097$

with $k_a=2,\ k_b=1$ and $M_a=1,\ M_b=2.$

Loading this model into the symbolic manipulation routines the explicit symbolic form of the symmetrized generalised FRF's up to the fifth order, are produced from an evaluation of equations (21), (26) and (27) as

$$H_1^{sym}(j\omega_1)=\frac{\alpha_{0,1}(0)}{\beta_{0,0}-\alpha_{1,0}(1)e^{-j\omega_1}-\alpha_{1,0}(2)e^{-j2\omega_1}} \tag{50}$$

$$H_2^{sym}(j\omega_1,j\omega_2)=0 \tag{51}$$

$$\begin{aligned}H_3^{sym}(j\omega_1,\ldots,j\omega_3)=&-\Big(\Big[\beta_{2,0}(0,0)+\beta_{2,0}(1,0)\left(e^{-j\omega_1}+e^{-j\omega_2}+e^{-j\omega_3}\right)/3\Big]\\&H_1(j\omega_1)H_1(j\omega_2)H_1(j\omega_3)\Big)/\\&\left(\beta_{0,0}-\alpha_{1,0}(1)e^{-j(\omega_1+\omega_2+\omega_3)}-\alpha_{1,0}(2)e^{-j2(\omega_1+\omega_2+\omega_3)}\right)\end{aligned} \tag{52}$$

$$H_4^{sym}(j\omega_1,\ldots,j\omega_4)=0 \tag{53}$$

$$\begin{aligned}H_5^{sym}(j\omega_1,\ldots,j\omega_5)=\Big(&-\Big(\beta_{2,0}(0,0)\big(H_1(j\omega_4)H_1(j\omega_5)H_3(j\omega_1,j\omega_2,j\omega_3)+\\&H_1(j\omega_1)H_1(j\omega_5)H_3(j\omega_2,j\omega_3,j\omega_5)+\\&H_1(j\omega_1)H_1(j\omega_2)H_3(j\omega_3,j\omega_4,j\omega_5)\big)\Big)\\&-\beta_{2,0}(1,0)\Big(\Big(\left(e^{-j\omega_1}+e^{-j\omega_2}+e^{-j\omega_3}+e^{-j\omega_4}+e^{-j\omega_5}\right)H_1(j\omega_4)\\&H_1(j\omega_5)H_3(j\omega_1,j\omega_2,j\omega_3)\Big)/5+\\&\left(\left(e^{-j\omega_1}+e^{-j\omega_2}+e^{-j\omega_3}+e^{-j\omega_4}+e^{-j\omega_5}\right)H_1(j\omega_1)\right.\\&\left.H_1(j\omega_5)H_3(j\omega_2,j\omega_3,j\omega_4)\right)/5+\\&\Big(\Big(e^{-j(\omega_1+\omega_2+\omega_3)}+e^{-j(\omega_1+\omega_2+\omega_4)}+e^{-j(\omega_1+\omega_3+\omega_4)}+e^{-j(\omega_2+\omega_3+\omega_4)}+e^{-j(\omega_1+\omega_2+\omega_5)}\\&e^{-j(\omega_1+\omega_3+\omega_5)}+e^{-j(\omega_2+\omega_3+\omega_5)}+e^{-j(\omega_1+\omega_4+\omega_5)}+e^{-j(\omega_2+\omega_4+\omega_5)}+e^{-j(\omega_3+\omega_4+\omega_5)}\Big)\\&H_1(j\omega_1)H_1(j\omega_2)H_3(j\omega_3,j\omega_4,j\omega_5)\Big)/10\Big)\Big)/\\&\left(\beta_{0,0}-\alpha_{1,0}(1)e^{-j(\omega_1+\omega_2+\omega_3+\omega_4+\omega_5)}-\alpha_{1,0}(2)e^{-j2(\omega_1+\omega_2+\omega_3+\omega_4+\omega_5)}\right)\end{aligned} \tag{54}$$

These expressions reveal how each time domain model term influences the generalised FRFs and if required they can be numerically evaluated by sweeping each frequency variable over some defined range to yield the traditional plots of gain and phase. The response of the first order FRF, which only depends on the linear terms eqn(50) are plotted

in figures *2a* and *2b*. These show a resonant peak at a frequency of 0.01518 rad/s. The inverse tangent in eqn(40) which used to compute the phase angle is wrapped in the range of $[-180^o, 180^o]$ as in figure *2b*. Applying eqn(42) yields the unwrapped phase illustrated in figure *2c* which is much easier to interpret.

The second order generalised FRF's is zero because when n=2 there are no terms which make a contribution to $H_2(j\omega_1, j\omega_2)$.

Now consider a slice of the third the order FRF $H_3(j\omega_1, j\omega_2, j\omega_3)$, which is illustrated in figure *3a* for the region $0 \le \omega_1 \le 0.06$ and $-0.06 \le \omega_1 \le 0.06$. Figure *3a* shows a number of resonant peaks and ridges which can also be seen in the corresponding contour plot of figure *3b* for $\omega_3 = \omega_1$. The ridges are generated whenever one of the factors $H_1(\bullet)$ in the numerator of eqn(52) is excited at 0.01518 rad/s the linear resonant frequency and the peaks occur when this is true for all three factors(see the dotted lines in figure *3b*). However, the plots seem to be very complicated and which model parameters contribute to the formation of which peaks, ridges or valleys is not apparent. Symbolic processing the third order FRF in eqn(52) using the results of equations (38) and (39) with $\omega_3 = \omega_1$ simplifies the analysis further.

The complete third order FRF is now easier to understand because it can be decomposed into the addition of individual contributing effects. Each of these effects can be graphed as shown in figures *4a, b, c, d* and *e* which make-up the total magnitude of the FRF in figure *3a*. The original phase plot shown in figures *3c* and *3d* exhibits the usual discontinuities which make it difficult to interpret. The unwrapped phase is illustrated in figures *3e* and *f*. The individual components which contribute to figure *3e* are shown in figures *5a, c, e, g* and *i*. Inspection of the components revealed by the symbolic processing aids the interpretation of $H_3(j\omega_1, j\omega_2, j\omega_3)$. Figure *4a* shows that the effect of the parameter $\alpha_{0,1}(0)$ is to lower the magnitude of $H_3(\bullet)$ by a constant amount of -360dB. $H_3(j\omega_1, j\omega_2, j\omega_3)$ will therefore be negligible compared with the first order FRF under normal operation of the system. This parameter has no affect on the phase which for this term will be zero. The contribution of the phase angle 180^o in the phase plots of the FRF's in figure *5a* comes from the minus sign in $H_3(\bullet)$as indicated in the symbolic expression eqn(52). The ridges in figure *4b* and figure *4c* are formed by the dimensional extention of the first order frequency response functions, $H_1(j\omega_1)$ and $H_1(j\omega_2)$ which covers the frequency range $(-0.06, 0.06)$ and $(0, 0.06)$ respectively. Clearly the model parameters in eqn(49) have a direct influence on the shape of the FRF's in figures *4b, 4c* and *4d*. The magnitude plots in figure *4d* exhibit two distinct ridges and by graphical measurement, these ridges correspond to the output frequency $\omega_{out} = \omega_1 + \omega_2 = \pm 0.01518$ rad/s. Thus,

significant non-linear characteristics. Analysis shows that these effects are negligible for this system.

7.3 A Non-linear Integro-Differential Equation Example

This class of models includes systems of the following form(Adamopoulos and Hammond,1988) with the inclusion of a constant term

$$D^2y(t)+0.1Dy(t)-0.1y(t)+y(t)^3-10-u(t)=0 \tag{62}$$

where from eqn(28)

$c_{1,0}(2)=1.0$ $\quad c_{1,0}(1)=0.1$ $\quad c_{1,0}(0)=-0.1$

$c_{3,0}(0,0,0)=1.0$ $\quad c_0=-10$ $\quad c_{0,1}(0)=-1.0$ $\quad else \quad c_{p,q}(\bullet)=0;$

The behaviour of the process can be analysed using the non-linear transfer function approach using the recursive relationship given in section 4.0.

The symmetrized generalized FRF's, up to fifth order, can be obtained for this model symbolically using equation (32) and converted to symmetrical form using equations (26) and (27) to yield

$$H^{sym}{}_1(j\omega_1)=-\frac{c_{0,1}(0)}{c_{1,0}(0)+(j\omega_1)c_{1,0}(1)+(j\omega_1)^2c_{1,0}(2)+3H_0{}^2c_{3,0}(0,0,0)} \tag{63}$$

$$H^{sym}{}_2(j\omega_1,j\omega_2)=-\frac{3H_0\,c_{3,0}(0,0,0)H_1(j\omega_1)H_1(j\omega_2)}{c_{1,0}(0)+(j\omega_1+j\omega_2)c_{1,0}(1)+(j\omega_1+j\omega_2)^2c_{1,0}(2)+3H_0{}^2c_{3,0}(0,0,0)} \tag{64}$$

$$H^{sym}{}_3(j\omega_1,j\omega_2,j\omega_3)=-\frac{\left(c_{3,0}(0,0,0)(H_1(j\omega_1)H_1(j\omega_2)H_1(j\omega_3)+3H_0H_1(j\omega_3)H_2(j\omega_1j\omega_2)+3H_0H_1(j\omega_1)H_2(j\omega_2j\omega_3)\right)}{c_{1,0}(0)+(j\omega_1+j\omega_2+j\omega_3)c_{1,0}(1)+(j\omega_1+j\omega_2+j\omega_3)^2c_{1,0}(2)+3H_0{}^2c_{3,0}(0,0,0)} \tag{65}$$

$$H^{sym}{}_4(j\omega_1,\ldots,j\omega_4)=-\frac{\left(c_{3,0}(0,0,0)\left(H_1(j\omega_3)H_1(j\omega_4)H_2(j\omega_1,j\omega_2)+H_1(j\omega_1)H_1(j\omega_4)H_2(j\omega_2,j\omega_3)+H_1(j\omega_1)H_1(j\omega_2)H_2(j\omega_3,j\omega_4)+3H_0H_2(j\omega_1,j\omega_2)H_2(j\omega_3,j\omega_4)+3H_0H_1(j\omega_4)H_3(j\omega_1,j\omega_2,j\omega_3)+3H_0H_1(j\omega_1)H_3(j\omega_2,j\omega_3,j\omega_4)\right)\right)}{c_{1,0}(0)+(j\omega_1+j\omega_2+j\omega_3+j\omega_4)c_{1,0}(1)+(j\omega_1+j\omega_2+j\omega_3+j\omega_4)^2c_{1,0}(2)+3H_0{}^2c_{3,0}(0,0,0)} \tag{66}$$

$$\begin{aligned}H^{sym}{}_5(j\omega_1,\ldots,j\omega_5)=-\big(&c_{3,0}(0,0,0)\big(H_1(j\omega_5)H_2(j\omega_1,j\omega_2)H_2(j\omega_3,j\omega_4)\\&+H_1(j\omega_3)H_2(j\omega_1,j\omega_2)H_2(j\omega_4,j\omega_5)+H_1(j\omega_1)H_2(j\omega_2,j\omega_3)H_2(j\omega_4,j\omega_5)\\&+H_1(j\omega_4)H_1(j\omega_5)H_3(j\omega_1,j\omega_2,j\omega_3)+3H_0H_2(j\omega_4,j\omega_5)H_3(j\omega_1,j\omega_2,j\omega_3)\end{aligned}$$

The use of symbolic algebra in the computation, decomposition and analysis of generalised or higher order frequency response functions for both discrete time polynomial and rational NARMAX models and continuous time non-linear differential equations has been presented. The symbolic processing provides an analytic form for each frequency response function and allows the user to see how the complex peaks, ridges and valleys are produced by the time domain model terms and coefficients. Three examples have been discussed in detail to illustrate the application of the new algorithms.

Acknowledgements

One of the author, (SAB) gratefully acknowledges the support of SERC grant ref GR/J05149.

Both authors gratefully acknowledge Dr. R Jefferys of Conoco Ltd for supplying the TLP data and for all the help he provided during the analysis of this data.

References

ADAMOPOULOS, P.G. AND HAMMOND,J.K, 1988,Wigner-Ville distribution and pattern identification for non-linear systems, *6th IMAC Orlando*, pp1446-1452.

BEDROSIAN,E. AND RICE,S.O,1971,The output properties of Volterra systems (nonlinear systems with memory)driven by harmonic and gaussian inputs , *Proc IEEE*, Vol.59, pp. 1688-1707.

BILLINGS,S.A. AND CHEN, S.,1989, Identification of nonlinear rational systems using a predictive error estimation algorithms, *Int J. Systems Sci.*, Vol.20(4), pp. 467-494.

BILLINGS,S.A. AND PEYTON JONES, J.C,1990, Mapping non-linear integro-differential equation into the frequency domain, *Int J. Control*, Vol.52(4), pp. 863-879.

BILLINGS,S.A. AND ZHANG,H.,1994, Frequency domain effects of constant terms in non-linear models, *Research Report no. 524, Department of Automatic , Control and System Engineering, University of Sheffield, U.K.*

BILLINGS,S.A. AND ZHU,Q.M,1991, Rational model identification using an extended least squares algorithm, *Int J. Control*, Vol.54, pp. 529-546.

BILLINGS, S.A. AND ZHU,Q.M,1994, A structure detection algorithm for nonlinear dynamic rational model, *Int J. Control* (to appear)

BILLINGS,S.A. AND TSANG,K.M,1989a, Spectral analysis for nonlinear systems.Part I-Parametric nonlinear spectral analysis, *J. Mechanical Systems and Signal Processing*, Vol.3(4), pp. 341-359.

BILLINGS,S.A. AND TSANG,K.M,1989a, Spectral analysis for nonlinear systems.Part II-Interpretation of nonlinear frequency response functions, *J. Mechanical Systems and Signal Processing*, Vol.3(4), pp. 341-359.

CHEN,S. AND BILLINGS,S.A.,1989, Representation of nonlinear systems: The NARMAX model, *Int J. Control*, Vol.49(3), pp. 1013-1032.

CHO,,Y.S., KIM, S.B., HIXSON, E.L. AND POWERS, E.J., 1992, A digital technique to estimate second order distortion using higher order coherence spectra, *IEEE Transaction on Acoustic, Speech and Signal Processing*, Vol. 40(5), pp. 1029-1040.

CHUA,L.O. AND NG,C.Y.,1979a, Frequency domain analysis of nonlinear systems: General theory, *IEE Journal Electronic Circuits and Systems*, Vol.3(4), pp.165-185.

CHUA,L.O. AND NG,C.Y.,1979b, Frequency domain analysis of nonlinear systems: Formulation of transfer functions, *IEE Journal Electronic Circuits and Systems*, Vol.3(6), pp.257-269

EVANS,BRIAN.L.,KARAM,LINA J.,WEST,KEVIN A AND MCCELLAN,JAMES H. ,1993, Learning signals and systems with *Mathematica*, *IEEE Transaction of Education*, Vol.36(1), pp. 72-78.

JEFFERYS,E.J, BILLINGS, S.A, JAMALUDDIN, H., AND TOMLINSON, G.R., 1991 A non-linear discrete time model of the drift force, *Proc. Sixth Int. Workshop on Water Waves and Floating Bodies, Woods Hole.*

KIM,K.I. AND POWERS,E.J.,1988, A digital method of modelling quadratically non-linear systems with a general random input, *IEEE Transaction on Acoustic, Speech and Signal Processing*, Vol.36, pp.1758-1769.

MCGOWAN,R. AND KUC,R.,1982, A direct relation between a signal time series and its unwrapped phase: Theory, examples and program, *IEEE Transaction on Acoustic, Speech and Signal Processing*, Vol.30, *pp.719-726.*

NETHERY,J.F. AND SPONG, M.W., 1994, Robotica: A Mathematica package for Robot analysis, *IEEE Robotics & Automation magazine*, Vol. 1, No.1, pp13-40

PEYTON-JONES,J.C. AND BILLINGS, S.A.,1989, A recursive algorithms for computing the frequency response of a class of non-linear difference equation models, *Int J. Control*, Vol.50(5), pp. 1925-1940.

PEYTON-JONES,J.C. AND BILLINGS, S.A.,1992, Mean levels in non-linear analysis and identification, Research report no.454, *Department of Automatic Control and Systems Engineering*, University of Sheffield.

WIENER,N., 1942, Response of a nonlinear device to noise, Report no. 129, *Radiation Laboratory*, MIT

WOLFRAM,S., 1991, *Mathematica, A System for doing Mathematics by Computer*, Addison Wesley Publications.

TOMLINSON,G.R AND BILLINGS,S.A., 1991, Higher order frequency response functions in nonlinear system identification, *Int. Forum on Aeroelasticity and structural Dynamics*, Aachen, 3-6 June.

TRIBOLET,J.M.,1977, A new phase unwrapping algorithm, *IEEE Transaction on Acoustic, Speech and Signal Processing*, Vol.26, pp.170-177.

VINH,T.,CHOUYCHAI,T.,LIU,H., AND DJOUDER,M., 1987, Second order transfer function: Computation and physical interpretation, 5th *IMAC*, London.

ZHANG,H., AND BILLINGS, S.A.,1992 , Unwrapping the phase response functions for nonlinear system(Submitted for publication)

ZHANG,H., BILLINGS, S.A. AND ZHU,Q.M,1993, Frequency response functions for nonlinear rational models, *Int J. Control* (to appear)

Figure Captions

Figure 1: The n-th order transfer function

Figure 2: $H_1(j\omega_1)$ of the rational model eqn(49) (a) Magnitude response (b) Phase response (c) Unwrapped phase response

Figure 3: $H_3(j\omega_1, j\omega_2, j\omega_3)$ of the rational model eqn(49) (a) Magnitude response (b) Magnitude contour plot (c) Phase response (d) Phase contour plot (e) Unwrapped phase response (f) Unwrapped phase contour plot

Figure 4: Magnitude decomposition of $H_3(j\omega_1, j\omega_2, j\omega_3)$ for the rational model eqn(49)

Figure 5: Phase decomposition of $H_3(j\omega_1, j\omega_2, j\omega_3)$ for the rational model eqn(49) (a),(b),(d), (f) and (g) -Principal value of phase response (c),(e),(g) and (i) - Unwrapped phase response.

Figure 6: $H_1(j\omega_1)$ of the polynomial model eqn(55) (a) Magnitude response (b) Phase response

Figure 7: $H_2(j\omega_1, j\omega_2)$ of the polynomial model eqn(55) (a) Magnitude response (b) Magnitude contour plot (c) Phase response (d) Phase contour plot

Figure 8: $H_3(j\omega_1, j\omega_2, j\omega_3)$ of the polynomial model eqn(55) (a) Magnitude response (b) Magnitude contour plot (c) Phase response (d) Phase contour plot

Figure 9: $H_1(j\omega_1)$ of the NIDE model eqn(62) (a) Magnitude response (b) Phase response

Figure 10: $H_2(j\omega_1, j\omega_2)$ of the NIDE model eqn(62) (a) Magnitude response (b) Magnitude contour plot (c) Phase response (d) Phase contour plot

Figure 11: $H_3(j\omega_1, j\omega_2, j\omega_3)$ of the NIDE model eqn(62) (a) Magnitude response (b) Magnitude contour plot (c) Phase response (d) Phase contour plot

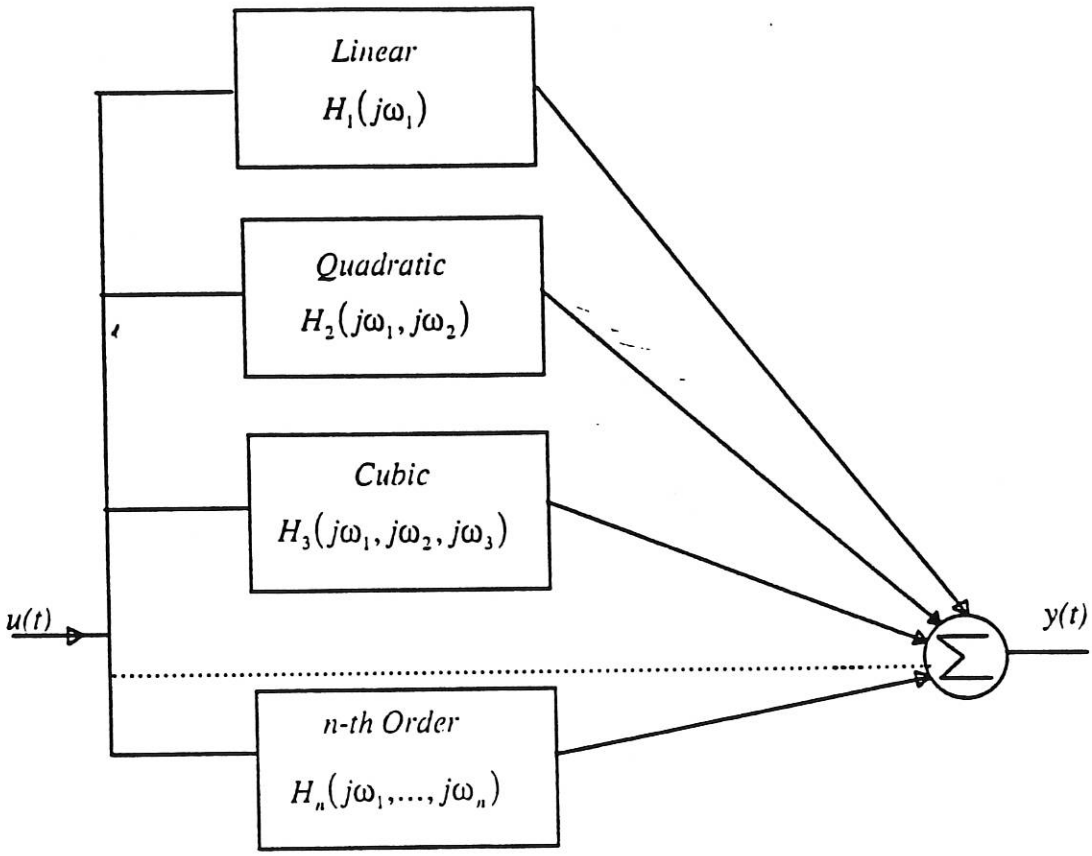

Figure 1: The n-th order transfer function

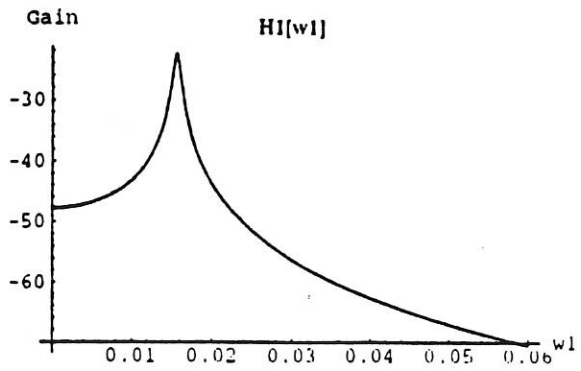

fig. 2a

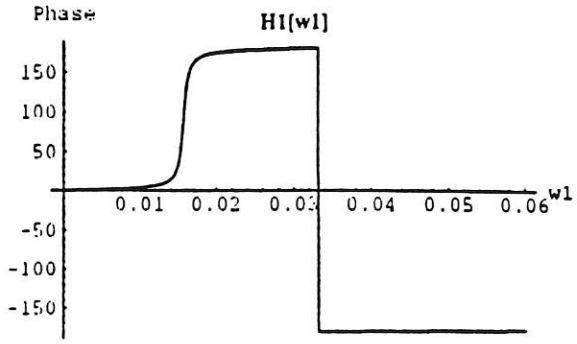

fig. 2b

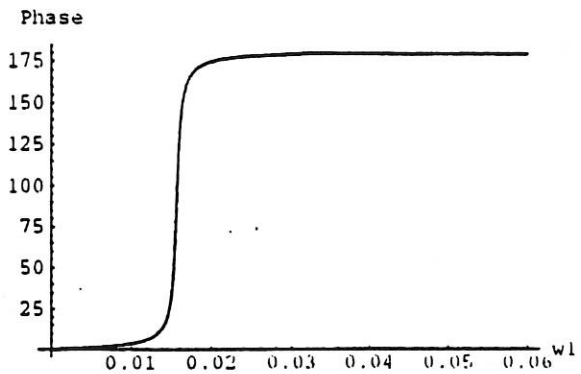

fig. 2c

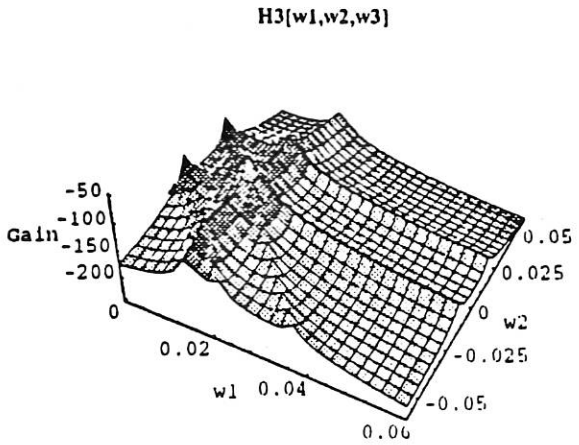

fig. 3a

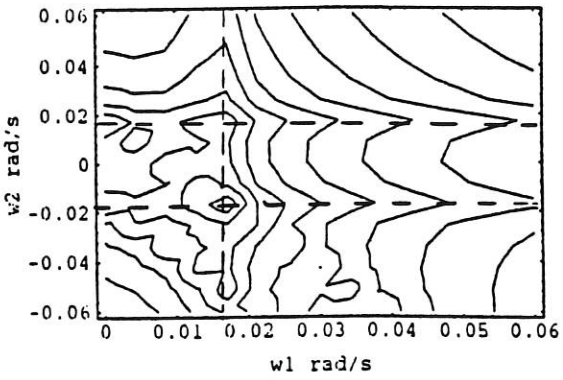

fig. 3b

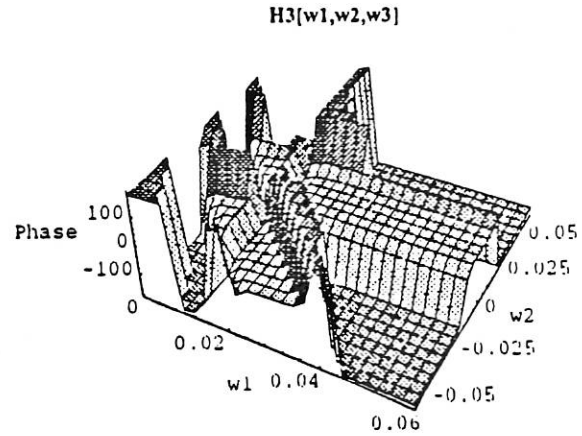

fig. 3c

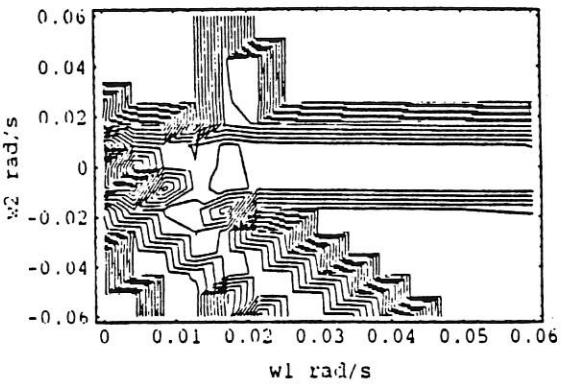

fig. 3d

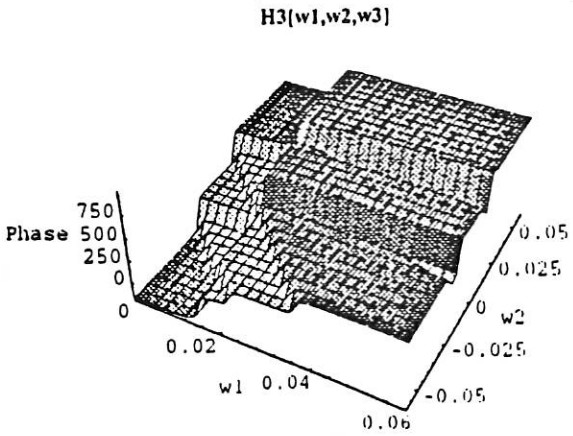

fig.3e

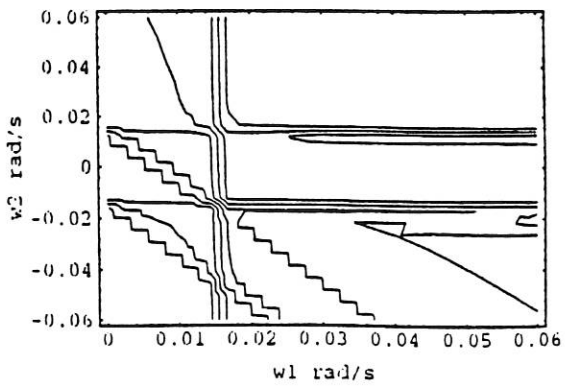

fig. 3f

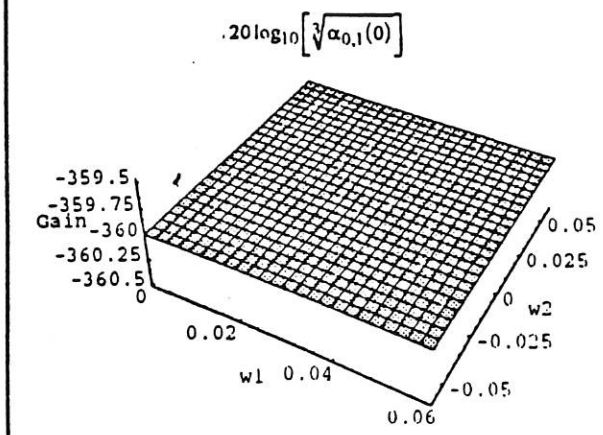

fig. 4a

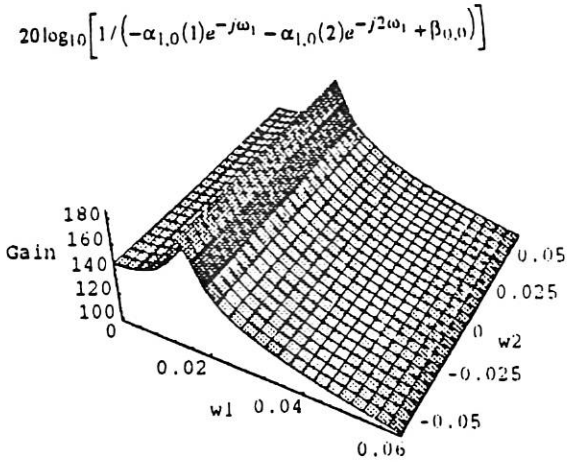

fig. 4b

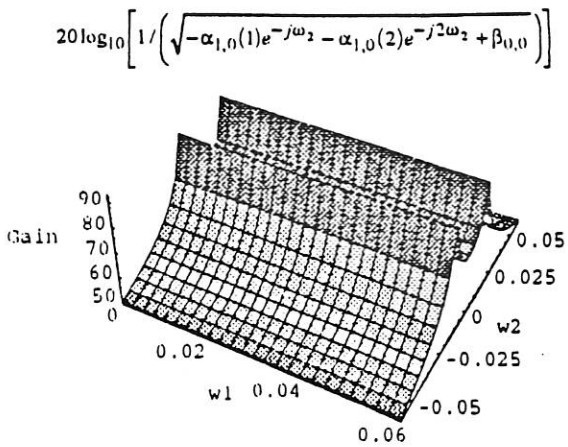

fig. 4c

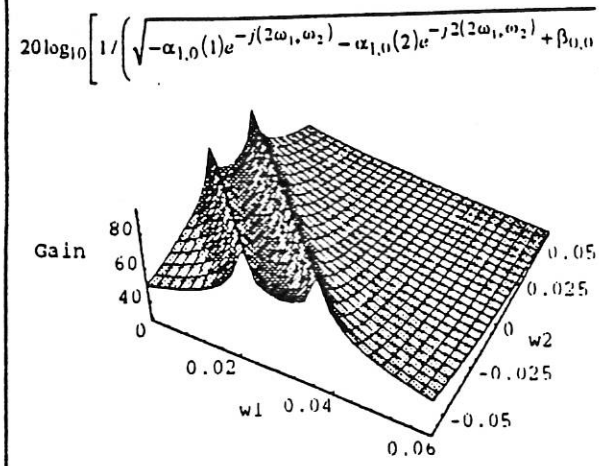

fig. 4d

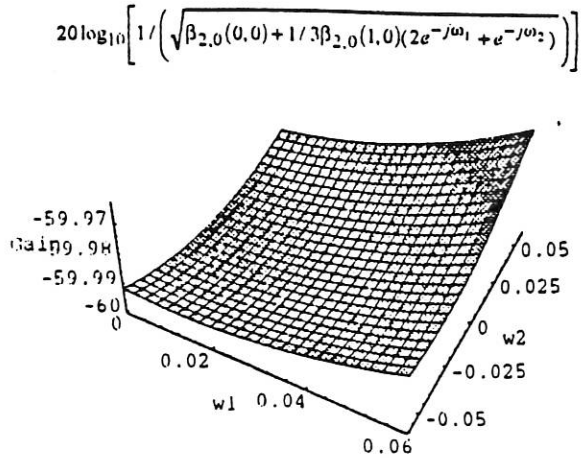

fig. 4e

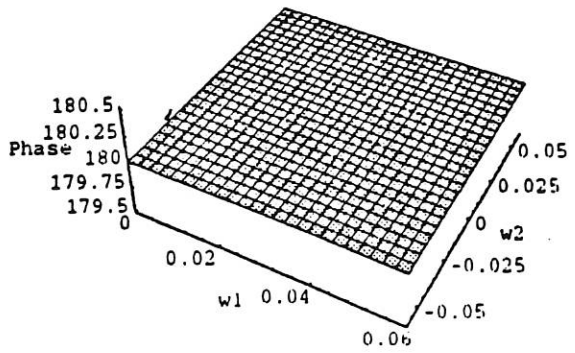

fig. 5a

$$180^{o}/\pi\times\left[1/\left(-\alpha_{1,0}(1)e^{-j\omega_1}-\alpha_{1,0}(2)e^{-j2\omega_1}+\beta_{0,0}\right)^{2}\right]$$

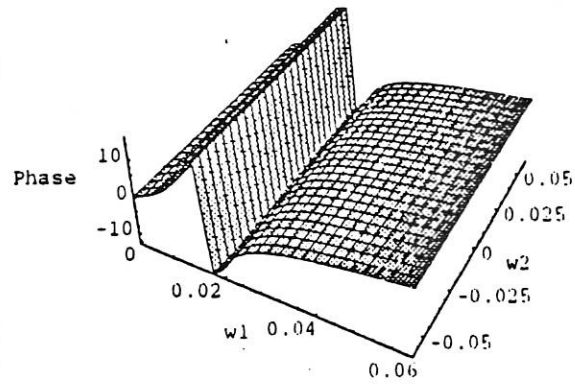

fig. 5b

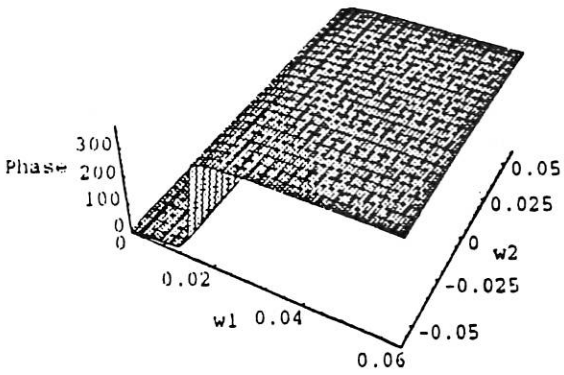

fig. 5c

$$180^{o}/\pi\times\left[1/\left(-\alpha_{1,0}(1)e^{-j\omega_2}-\alpha_{1,0}(2)e^{-j2\omega_2}+\beta_{0,0}\right)\right]$$

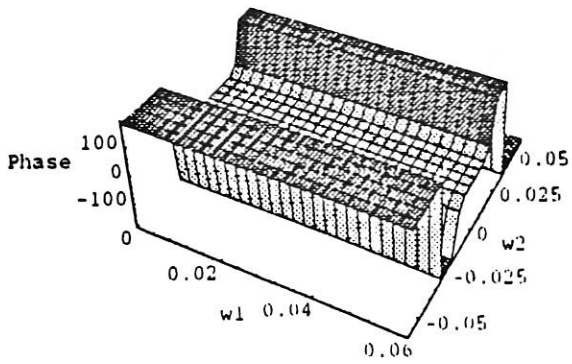

fig. 5d

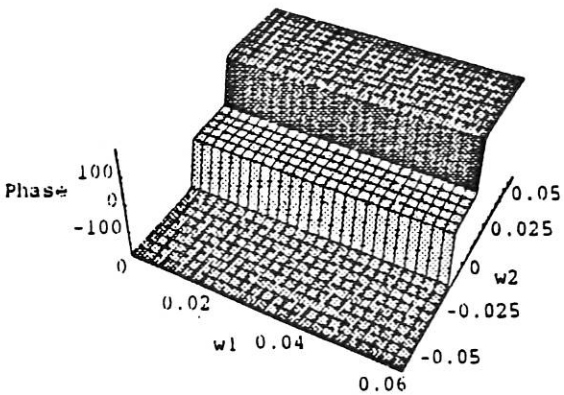

fig. 5e

$$180^{o}/\pi \times \left[1/\left(-\alpha_{1,0}(1)e^{-j(2\omega_1+\omega_2)} - \alpha_{1,0}(2)e^{-j2(2\omega_1+\omega_2)} + \beta_{0,0}\right)\right]$$

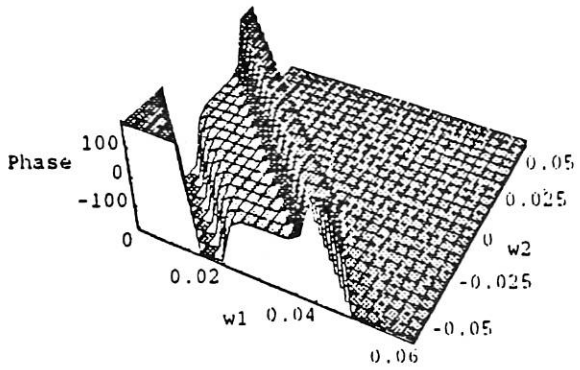

fig. 5f

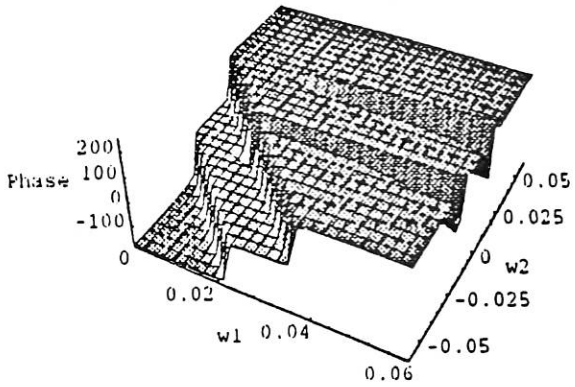

fig. 5g

$$180^{o}/\pi \times \arg\left[\beta_{2,0}(0,0) + 1/3\beta_{2,0}(1,0)(2e^{-j\omega_1} + e^{-j\omega_2})\right]$$

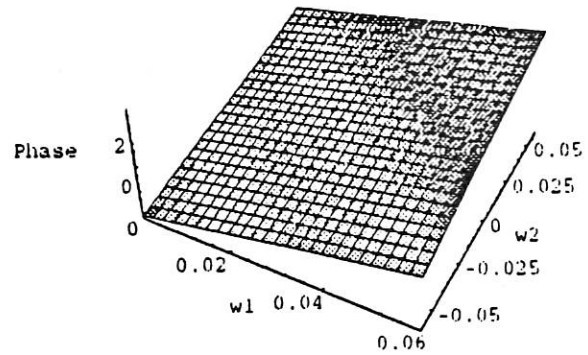

fig. 5h

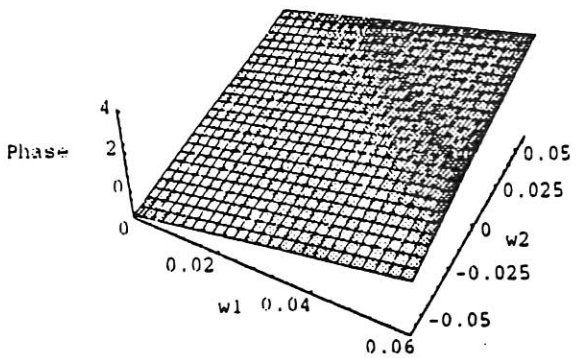

fig. 5i

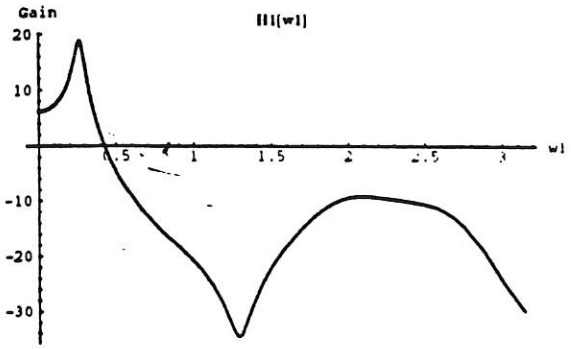

fig. 6a

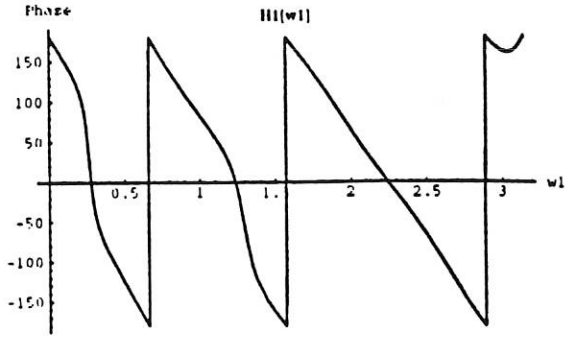

fig. 6b

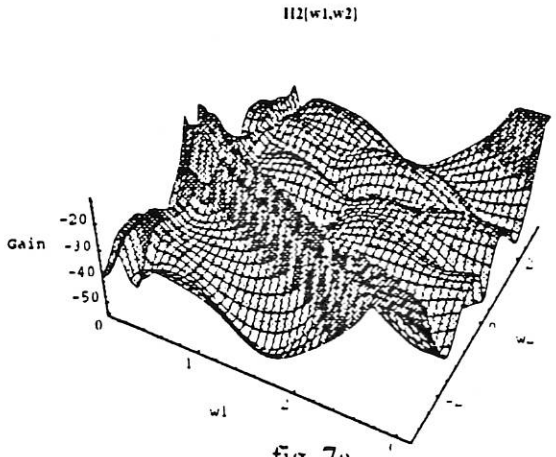

fig. 7a

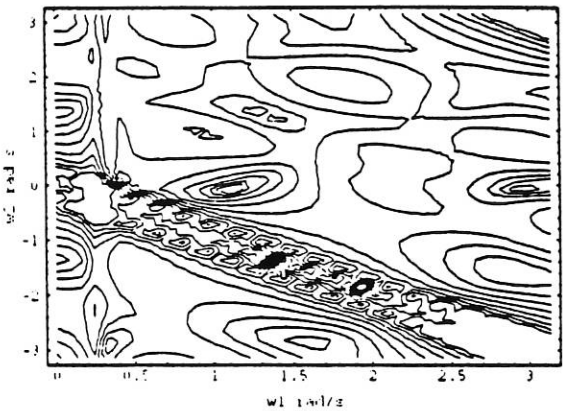

fig. 7b

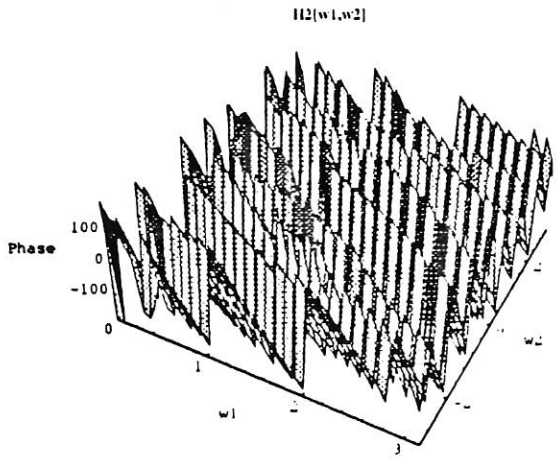

fig. 7c

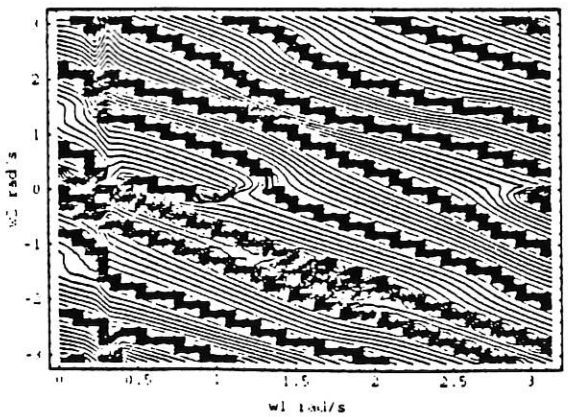

fig. 7d

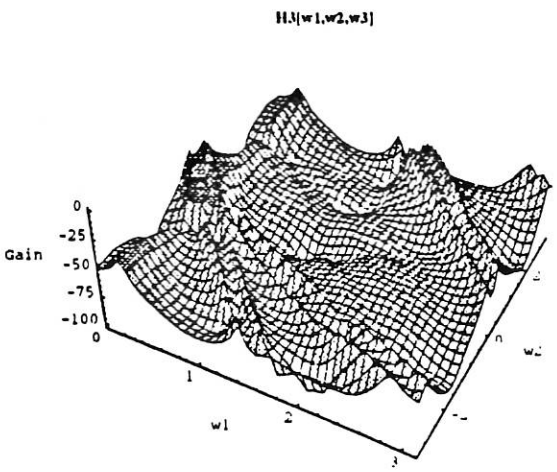

fig. 8a

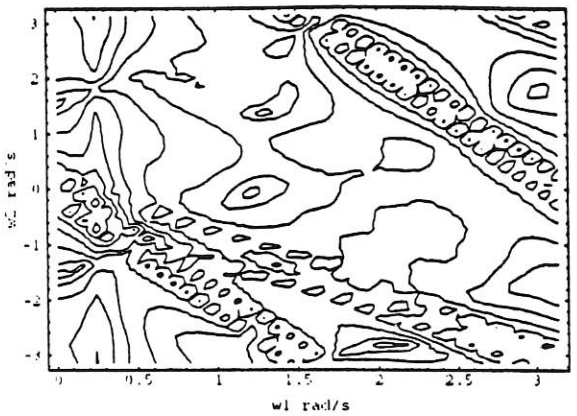

fig. 8b

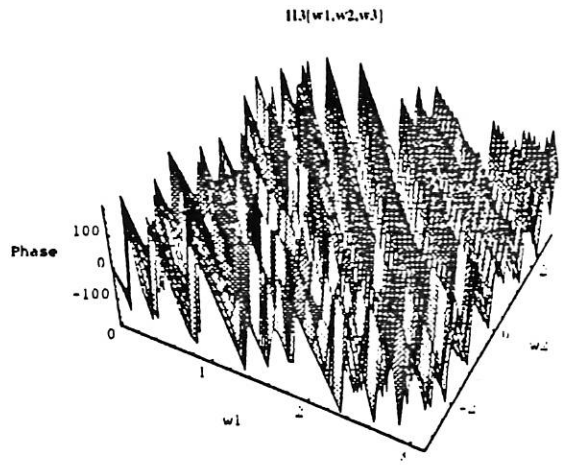

fig. 8c

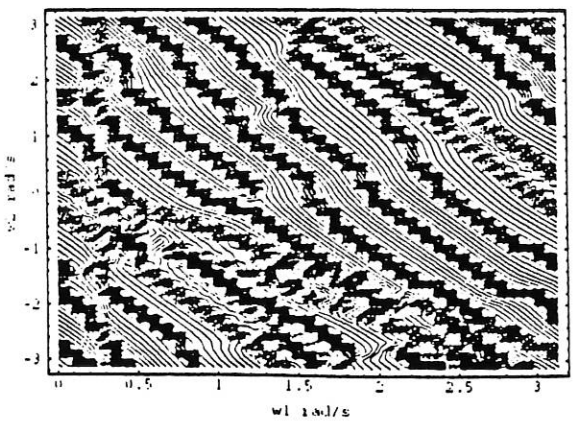

fig. 8d

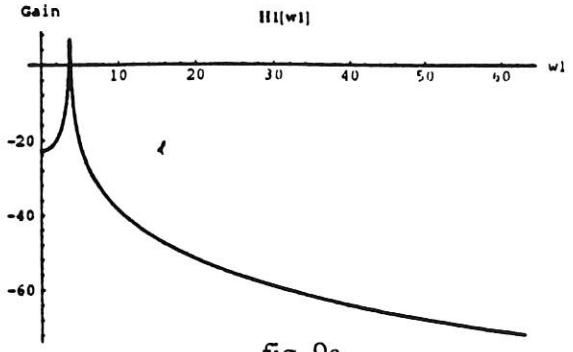

fig. 9a

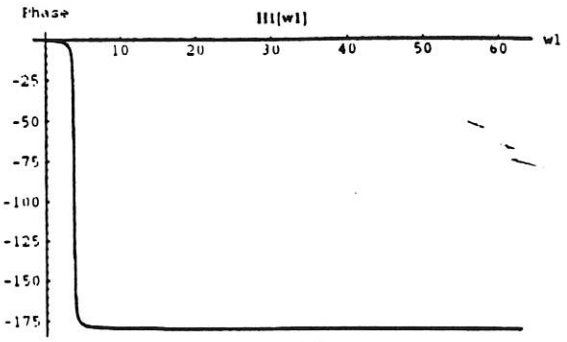

fig. 9b

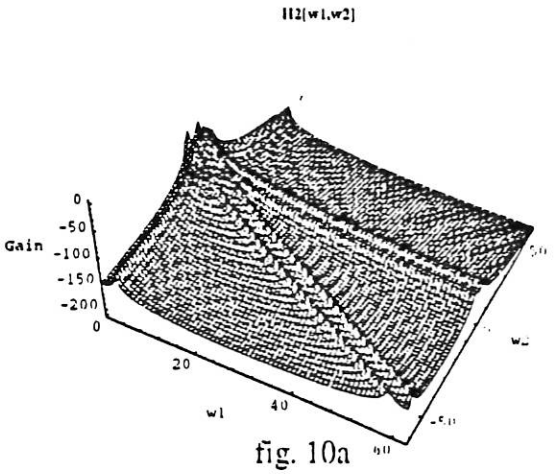

fig. 10a

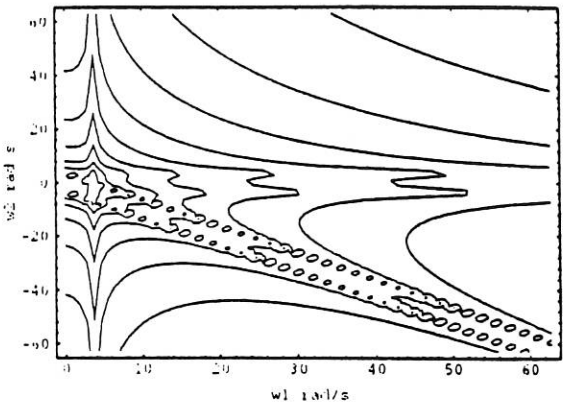

fig. 10b

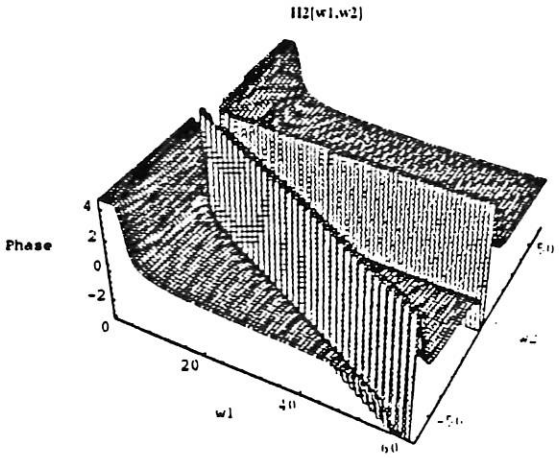

fig. 10c

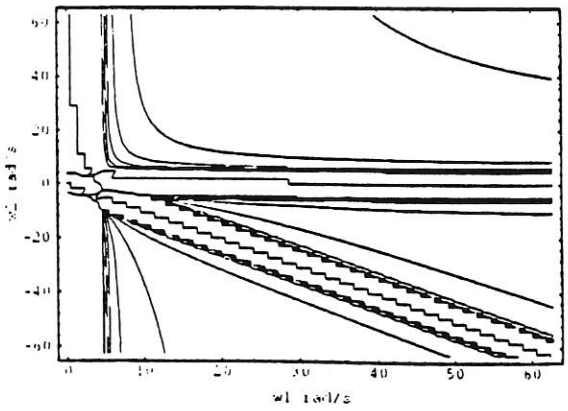

fig. 10d

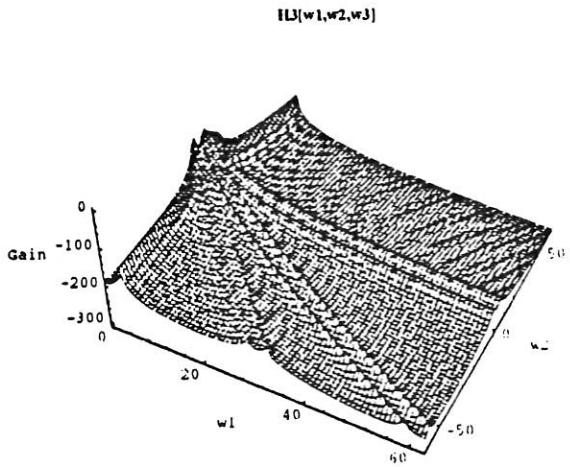

fig. 11a

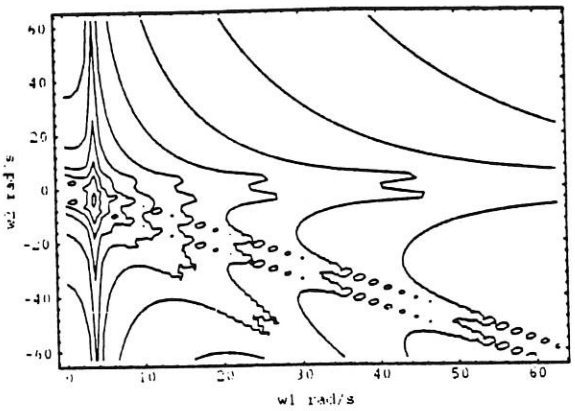

fig. 11b

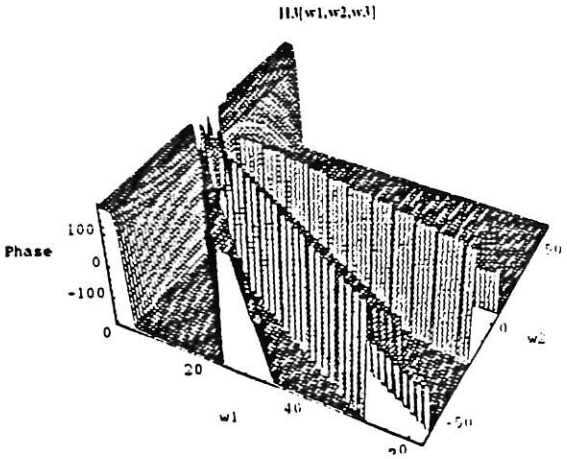

fig 11c

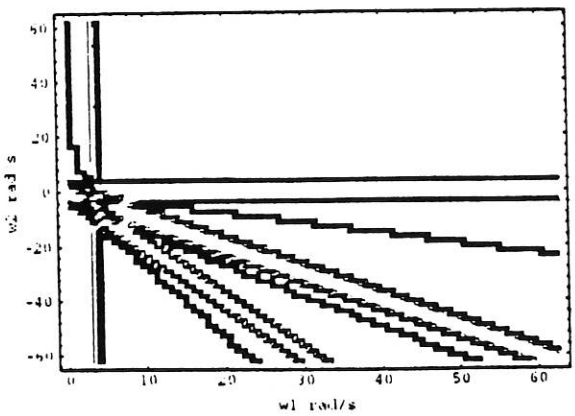

fig. 11d